The Journal of Antibiotics (2017) 70, 595–600

www.nature.com/ja

ORIGINAL ARTICLE

Antarlides F–H, new members of the antarlide family produced by *Streptomyces* sp. BB47

Shun Saito[1], Takahiro Fujimaki[1], Watanalai Panbangred[2], Ryuichi Sawa[3], Yasuhiro Igarashi[4] and Masaya Imoto[1]

Castration-resistant prostate cancer (CRPC) is the most aggressive form of this disease. CRPC remains dependent on androgen receptor (AR) signaling. Therefore, a novel AR antagonist, enzalutamide, is used clinically for the treatment of men with metastatic CRPC. However, enzalutamide-resistant AR has appeared, and a new type of AR antagonist is desired. Previously, in the course of screening for a new type of AR antagonist, we isolated a series of compounds, designated antarlides A–E, that share a novel 22-membered-ring macrocyclic structure and are produced by *Streptomyces* sp. BB47. In the present study, we found that this strain also produces antarlides F–H as minor components. Antarlide F is a novel geometric isomer of known antarlides. On the other hand, antarlides G and H are new members of the antarlide family that have a 20-membered-ring macrocyclic structure. Antarlides G and H inhibited the binding of androgen to AR *in vitro* at concentrations similar to those observed with antarlides A–E. In addition, antarlide G inhibited the transcriptional activity of not only wild-type AR but also enzalutamide-resistant AR, suggesting that antarlides with either 22- or 20-membered rings may serve as potent third-generation AR antagonists capable of overcoming resistance to enzalutamide.
The Journal of Antibiotics (2017) **70,** 595–600; doi:10.1038/ja.2017.6; published online 8 February 2017

INTRODUCTION

Prostate cancer is the second most common malignancy among men worldwide.[1] When an androgen (a male hormone) binds to the androgen receptor (AR), AR acts as a transcription factor and induces prostate tumor growth.[2] Therefore, androgen deprivation by medical or surgical castration is the standard first-line treatment for prostate cancer. However, most prostate cancer patients eventually acquire resistance to the treatments and develop a more aggressive form of the disease called castration-resistant prostate cancer (CRPC).[3] Persistent activation of the androgen–AR axis underlies resistance to androgen deprivation therapy and progression to metastatic CRPC.[4] The continued dependence on AR signaling in CRPC has led to the development of AR antagonists that compete with androgens for binding to the AR. MDV3100 (enzalutamide), a second-generation AR antagonist, has been approved for clinical use in men with metastatic CRPC.[5] However, recent studies have revealed that a F876L mutation in the AR confers resistance to enzalutamide, switching the antagonist to an agonist.[6]

Previously, we reported the isolation (from *Streptomyces* sp. BB47) and structural determination of antarlides A–E, a potent new generation of AR antagonists that overcomes resistance to enzalutamide.[7] Antarlides A–E are mutually isomeric with respect to the double bond and have a 22-membered-ring macrocyclic structure (Figure 1a). The full stereostructure of antarlide A was established by chemical modifications, including methanolysis, the Trost method, acetonide formation and the PGME (phenylglycine methyl ester) method. Antarlides A–E inhibit the binding of androgen to AR *in vitro*. In addition, antarlide B inhibited the transcriptional activity not only of wild-type AR but also of mutant ARs that are seen in patients with acquired resistance to clinically used AR antagonists.

Further analysis of the fermentation extract from *Streptomyces* sp. BB47, using LC-MS, revealed the presence of another three minor peaks showing the same MW and similar UV spectroscopic profiles as antarlides A–E. In the present study, we report the isolation, structural elucidation and AR antagonist activities of these three new antarlide analogs.

RESULTS AND DISCUSSION

Fermentation and isolation

Streptomyces sp. BB47 was cultured in A3MP production medium as described previously.[7] LC-MS analysis of the crude extract indicated the presence of three minor peaks displaying UV and MS spectra

[1]Department of Bioscience and Informatics, Faculty of Science and Technology, Keio University, Kanagawa, Japan; [2]Department of Biotechnology, Faculty of Science, Mahidol University, Bangkok, Thailand; [3]Institute of Microbial Chemistry (BIKAKEN), Tokyo, Japan and [4]Biotechnology Research Center, Toyama Prefectural University, Toyama, Japan
Correspondence: Professor Y Igarashi, Biotechnology Research Center, Toyama Prefectural University, Imizu, Toyama 939-0398, Japan.
E-mail: yas@pu-toyama.ac.jp
or Professor M Imoto, Department of Bioscience and Informatics, Faculty of Science and Technology, Keio University, 3-14-1 Hiyoshi, Kohoku-ku, Yokohama, Kanagawa 223-8522, Japan.
E-mail: imoto@bio.keio.ac.jp
The authors dedicate this work to Professor Satoshi Ōmura, a distinguished Novel Prize awardee in Physiology or Medicine 2015.
Received 24 October 2016; revised 8 December 2016; accepted 10 December 2016; published online 8 February 2017

similar to those of antarlides A–E (Figure 2). The corresponding fraction was subjected to two rounds of partitioning, one round of centrifugal liquid–liquid partition chromatography, and two rounds of HPLC purification. Processing from 12 L of culture yielded three new antarlide analogs: F (2.2 mg), G (1.6 mg) and H (1.0 mg). All isolation steps were carried out in the dark because these new antarlide analogs are also unstable under room light.

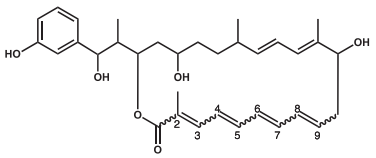

Antarlide

A : $\Delta^{2,3} = E$, $\Delta^{4,5} = E$, $\Delta^{6,7} = E$, $\Delta^{8,9} = E$
(11*S*, 16*R*, 19*S*, 21*S*, 22*R*, 23*R*)
B : $\Delta^{2,3} = E$, $\Delta^{4,5} = Z$, $\Delta^{6,7} = E$, $\Delta^{8,9} = Z$
C : $\Delta^{2,3} = E$, $\Delta^{4,5} = E$, $\Delta^{6,7} = Z$, $\Delta^{8,9} = Z$
D : $\Delta^{2,3} = E$, $\Delta^{4,5} = E$, $\Delta^{6,7} = Z$, $\Delta^{8,9} = E$
E : $\Delta^{2,3} = E$, $\Delta^{4,5} = Z$, $\Delta^{6,7} = E$, $\Delta^{8,9} = E$
F : $\Delta^{2,3} = Z$, $\Delta^{4,5} = E$, $\Delta^{6,7} = E$, $\Delta^{8,9} = E$

Figure 1-1. Structures of antarlide A-F

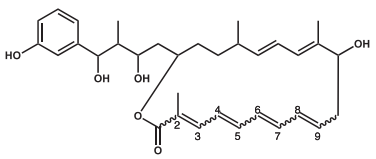

Antarlide

G : $\Delta^{2,3} = E$, $\Delta^{4,5} = Z$, $\Delta^{6,7} = E$, $\Delta^{8,9} = E$
H : $\Delta^{2,3} = E$, $\Delta^{4,5} = E$, $\Delta^{6,7} = Z$, $\Delta^{8,9} = E$

Figure 1-2. Structures of antarlide G-H

Figure 1 (**a**) Structures of antarlides A–F. (**b**) Structures of antarlides G–H.

Structure elucidation

Antarlide F was obtained as a pale yellow powder. High-resolution ESITOF MS suggested a molecular formula of $C_{33}H_{44}O_6$ ($[M\text{-}H]^-$ $m/z = 535.3062$), which is the same as the molecular formulae of antarlides A–E. The ^1H and ^{13}C NMR data were also similar to those of antarlides A–E. Analysis of the ^1H-^1H COSY, HMQC and HMBC data for antarlide F led to a planar structure identical to that of antarlides A–E (Table 1 and Supplementary Figure S7). HMBC correlations from H21 to C1 indicated a 22-membered-ring macrocyclic structure. The double-bond geometries of antarlide F were assigned by the analysis of NOESY correlations. Interestingly, C2–C3 double bond was assigned as *Z* on the basis of NOESY correlations for H2a-H3, different from that of antarlides A–E. Antarlides A–E are mutually isomerized by room light, as described previously.[7] Antarlides A–F also were mutually isomerized within 2 h of exposure to room light (Supplementary Figure S23). This observation suggested that antarlide F is likely to have the same absolute configurations as those in antarlide A.

Antarlide G was obtained as a pale yellow powder. High-resolution ESITOF MS suggested a molecular formula of $C_{33}H_{44}O_6$ ($[M\text{-}H]^-$ $m/z = 535.3061$), which is the same as the molecular formulae of antarlides A–F. The ^1H and ^{13}C NMR data were also similar to those of antarlides A–F. Analysis of the ^1H-^1H COSY, HSQC and HMBC data for antarlide G led to a planar structure identical to that of antarlides A–F, except for the position of the macrocyclic ring formation (Table 1 and Figure 3). Among the four oxygenated sp^3 methines in the antarlides, H21 shows the highest chemical shift in antarlides A–F due to the lactone formation. However, H19 shows the highest chemical shift among the oxymethine protons in antarlide G. Moreover, HMBC correlation from H19 to C1 was observed by using selective HMBC; increased HMBC sensitivity for correlating poorly resolved proton (Supplementary Figure S13).[8] Therefore, these results suggested that antarlide G has a 20-membered-ring macrocyclic structure. The double-bond geometries of antarlide G were assigned

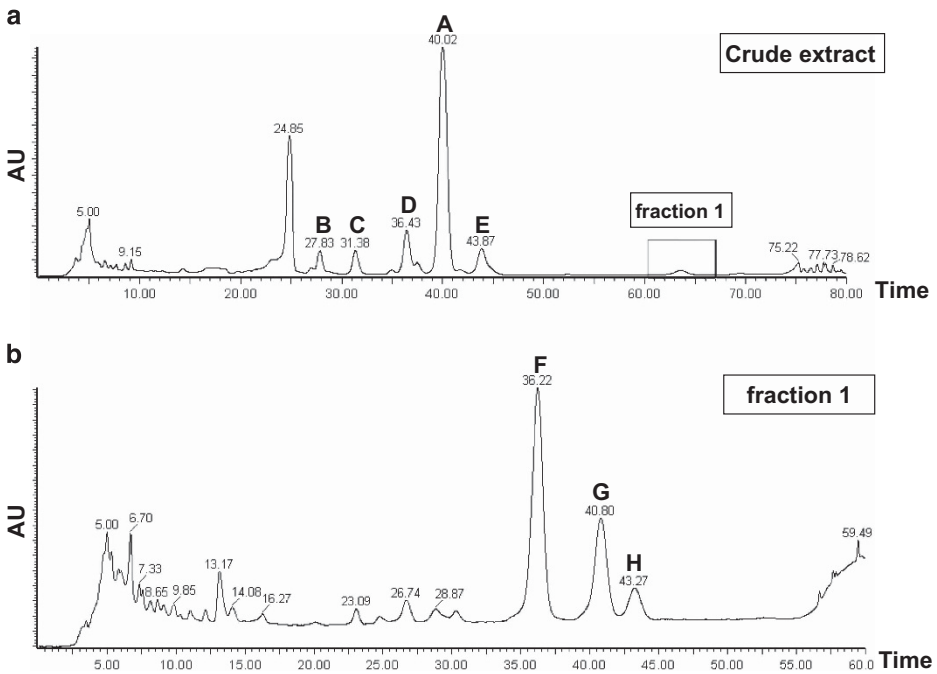

Figure 2 (**a**) Photodiode array (PDA) chromatogram of crude extract containing antarlides A–H (solvent: MeCN:H_2O = 1:1). (**b**) PDA chromatogram of fraction 1 containing antarlides F–H (solvent: MeOH:H_2O = 3:1).

Table 1 ^{1}H and ^{13}C NMR data for antarlides F–H in acetone-d_6

	Antarlide F		*Antarlide G*		*Antarlide H*	
Position	δ_C	δ_H *mult (J in Hz)*	δ_C	δ_H *mult (J in Hz)*	δ_C	δ_H *mult (J in Hz)*
1	168.7	—	167.1	—	167.7	—
2	127.8	—	127.3	—	126.9	—
2a	20.3	1.98 (3H, s)	11.8	1.91 (3H, s)	12.0	1.89 (3H, s)
3	137.2	6.51 (1H, d, 11.3)	131.5	7.65 (1H, d, 12.2)	138.9	7.18 (1H, d, 11.4)
4	129.6	7.21 (1H, dd, 11.5, 15.1)	123.3	6.31 (1H, m)	127.3	6.56 (1H, dd, 11.7, 14.4)
5	136.0	6.36 (1H, dd, 10.1, 14.8)	135.2	6.39 (1H, m)	135.7	6.82 (1H, m)
6	130.5	6.12 (1H, dd, 10.1, 15.0)	125.4	6.62 (1H, dd, 11.7, 15.2)	134.0	6.08 (1H, m)
7	124.3	6.27 (1H, m)	136.2	6.34 (1H, m)	126.7	6.10 (1H, m)
8	132.6	6.02 (1H, m)	131.1	6.26 (1H, m)	125.1	6.71 (1H, m)
9	130.4	5.71 (1H, ddd, 6.4, 7.9)	131.4	5.90 (1H, ddd, 5.0, 15.2)	134.0	5.91 (1H, ddd, 4.8, 15.9)
10	36.5	2.43 (2H, m)	35.3	2.48 (2H, m)	35.8	2.57 (2H, m)
11	75.1	4.17 (1H, m)	74.9	4.36 (1H, m)	75.3	4.43 (1H, dt, 0.3, 7.0)
12	136.3	—	137.0	—	138.3	—
12a	12.6	1.69 (3H, s)	11.1	1.71 (3H, s)	10.3	1.71 (3H, s)
13	126.3	6.02 (1H, m)	127.9	6.24 (1H, m)	128.9	6.41 (1H, m)
14	133.6	6.27 (1H, m)	123.5	(1H, dd, 10.5, 15.5)	123.7	6.42 (1H, m)
15	140.0	5.60 (1H, dd, 7.2, 15.2)	138.9	5.97 (1H, dd, 5.6, 15.1)	138.5	6.25 (1H, dd, 3.9, 14.2)
16	36.5	2.25 (1H, m)	35.9	2.22 (1H, m)	34.6	2.19 (1H, m)
16a	19.2	1.06 (3H, d, 6.8)	19.0	1.09 (3H, d, 6.7)	19.0	1.10 (3H, d, 6.7)
17	33.5	1.40, 1.56 (2H, m)	35.3	1.33, 1.41 (2H, m)	35.1	1.22, 1.45 (2H, m)
18	35.6	1.40, 1.55 (2H, m)	32.1	1.77, 1.92 (2H, m)	32.2	1.83 (2H, m)
19	68.6	3.68 (1H, m)	73.4	5.02 (1H, m)	73.4	4.89 (1H, m)
20	40.7	1.78, 1.99 (2H, m)	39.1	1.68, 2.00 (2H, m)	39.6	1.65, 2.05 (2H, m)
21	72.5	5.82 (1H, m)	68.0	4.13 (1H, m)	68.2	4.14 (1H, m)
22	44.0	2.05 (1H, m)	44.5	1.87 (1H, m)	44.7	1.85 (1H, m)
22a	10.0	0.69 (3H, d, 6.9)	10.7	0.77 (3H, d, 7.2)	10.9	0.77 (3H, d, 7.1)
23	75.5	4.17 (1H, m)	76.8	4.57 (1H, m)	77.0	4.57 (1H, m)
24	146.1	—	146.7	—	147.0	—
25	114.2	6.84 (1H, t, 1.85)	113.5	6.89 (1H, s)	113.8	6.88 (1H, s)
26	157.6	—	157.3	—	157.5	—
27	114.4	6.72 (1H, dd, 2.7, 7.9)	113.8	6.72 (1H, dd, 2.4, 7.9)	114.1	6.71 (1H, m)
28	129.1	7.12 (1H, t, 7.8)	128.9	7.14 (1H, t, 8.0)	129.1	7.14 (1H, t, 7.8)
29	118.6	6.78 (1H, d, 7.4)	117.7	6.81 (1H, d, 8.0)	118.0	6.82 (1H, m)

*The shaded chemical shift values are position of ring formation.

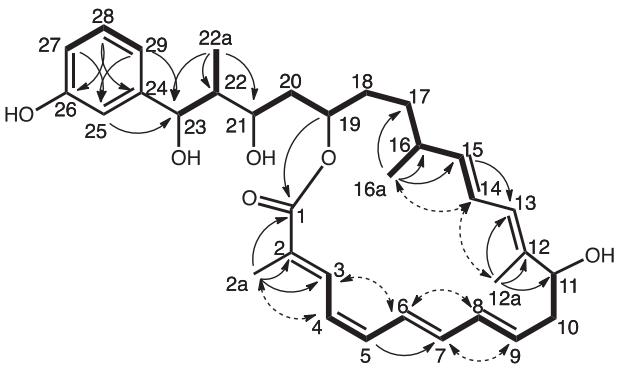

Figure 3 COSY (bold), key HMBC (arrow) and key NOESY (dashed arrow) correlations for antarlide G.

by analysis of NOESY correlations as shown in Figure 3. C2–C3, C4–C5, C6–C7, C8–C9, C12–C13 and C14–C15 double bonds were assigned as *E*, *Z*, *E*, *E*, *E* and *E*, respectively.

Antarlide H was obtained as a pale yellow powder. High-resolution ESITOF MS indicated a molecular formula of $C_{33}H_{44}O_6$ ([M-H]$^-$ m/z=535.3061), which is the same as the molecular formulae of antarlides A–G. The ^{1}H and ^{13}C NMR data were also similar to those of antarlides A–G. Analysis of the ^{1}H-^{1}H COSY, HMQC and HMBC data for antarlide H led to a planar structure identical to that of antarlide G (Table 1 and Supplementary Figure S22). Among the four oxygenated sp^3 methines, the chemical shift value of H19 is the highest. In addition, HMBC correlation from H19 to C1 was also observed by using selective HMBC (Supplementary Figure S20). These observations suggested that antarlide H also has a 20-membered-ring macrocyclic structure. The double-bond geometries of antarlide H were assigned by the analysis of NOESY correlations (Supplementary Figure S22). These double-bond geometries were the same as antarlide D, meaning that antarlide H is a geometric isomer of antarlide G. However, antarlide G and antarlide H are not mutually isomerized, although these compounds are isomerized to other antarlide analogs displaying UV and MS spectra similar to antarlides following exposure to room light (data not shown). In addition, antarlide G is more stable than antarlide H in room light.

Antarlides A–F, which have a 22-membered-ring macrocyclic structure, are mutually isomerized by room light, and antarlide A is the main product in the culture. Therefore, we speculate that *Streptomyces* sp. BB47 produces antarlide A as a 'natural product',

with conversion of antarlide A to antarlides B–F during bacterial cultivation and/or compound isolation. However, antarlides G and H are not generated from antarlide A under room light (data not shown). Therefore, it is likely that when the polyketide chain is cleaved and the lactone linkage is formed, fluctuation of substrate recognition by a thioesterase leads to the production of 20- and 22-membered macrocycles in *Streptomyces* sp. BB47.

Biological activities

Antarlides F–H were examined for their AR-DHT (AR-dihydrotestosterone) binding inhibition activities *in vitro*. Antarlides F–H inhibited the binding of AR-DHT at concentrations similar to those of antarlides A–E (Table 2). In addition, antarlides F–H did not inhibit ER–estradiol binding. These data suggested that the double-bond geometries and the ring size of the antarlides have no effect on the binding to AR and ER.

Emergence of a mutant AR has been shown to be linked to resistance to AR antagonists; recently, an F876L missense mutation in the AR was shown to confer resistance to the second-generation AR antagonist enzalutamide.[6] Previously, we reported that antarlide B inhibited DHT-induced transcriptional activity not only of the wild-type AR but also of the F876 mutant AR, indicating that antarlide B can overcome resistance to AR antagonists. We next examined whether antarlides having 20-membered-ring macrocyclic structures can overcome resistance to AR antagonists. Antarlide G inhibited the DHT-induced transcriptional activity of wild-type and mutant (F876L) AR at same concentration as that of antarlide B (Figure 4).

The mutant AR (F876L) confers antagonist to agonist for enzalutamide, and shows resistance. To check whether antarlide G shows agonist activity for both the wild-type and mutant ARs, we evaluated the effect of antarlide G on nuclear translocation of AR. Antarlide G did not induce nuclear translocation of either wild-type or mutant AR (Figure 5). Therefore, antarlide G did not show the agonist activity for either wild-type and mutant (F876L) AR. These data suggested that antarlide G overcomes resistance to enzalutamide.

In conclusion, we have discovered antarlides F–H, new members of the antarlide family of compounds produced by *Streptomyces* sp. BB47.

Table 2 IC_{50} values (μM) for the inhibition of binding of DHT to AR or estradiol to ER

Compound	*B*	*F*	*G*	*H*	*HF*[a]
AR	14	15	15	14	18
ER	>100	>100	>100	>100	>100

[a]HF, hydroxyflutamide, existing drug.

Antarlides F–H specifically inhibited AR-DHT binding. In addition, antarlide G, which possesses a 20-membered-ring macrocyclic structure, also inhibited the transcriptional activity of wild-type and mutant (F876L) AR with a potency to similar to that of antarlide B, which has a 22-membered-ring macrocyclic structure. These data suggested that the double-bond geometries and the ring sizes of the antarlides have no effect on these activities. Therefore, these novel antarlides may have utility as novel AR antagonists.

METHODS

General experimental procedures

Optical rotation was measured using a JASCO P-1020 polarimeter (JASCO Corporation, Tokyo, Japan). UV spectrum was recorded on a Beckman DU530 UV/VIS spectrophotometer (Beckman, Mississauga, ON, Canada). IR spectrum was measured on a JASCO RT/IR-4200 (JASCO Corporation). NMR spectra were obtained on a Bruker AVANCE 500 spectrometer (Bruker Biospin K. K., Kanagawa, Japan; antarlide G) or JEOL JNM-ECA500 spectrometer (antarlide F and H). HR-ESITOF MS was recorded on a LCT premier EX spectrometer (Waters Corporation, Milford, MA, USA). Selective HMBC spectra were obtained on a JEOL JNM-ECZ600R spectrometer with Ultra COOL probe (antarlide G and H).

Producing microorganism

The taxonomic characterization of strain BB47 was described previously.[9]

Fermentation

Strain BB47 cultured on a Bn-2 slant agar medium (soluble starch 0.5%, glucose 0.5%, meat extract (Kyokuto Pharmaceutical Industrial) 0.1%, yeast extract (Difco Laboratories, Sparks, MD, USA) 0.1%, NZ-case (Wako Pure Chemical Industries) 0.2%, NaCl 0.2%, $CaCO_3$ 0.1% and agar 1.5%) was inoculated into 500-ml Erlenmeyer flasks each containing 100 ml of V-22 seed medium (soluble starch 1%, glucose 0.5%, NZ-case 0.3%, yeast extract 0.2%, tryptone (Difco Laboratories) 0.5%, K_2HPO_4 0.1%, $MgSO_4{\cdot}7H_2O$ 0.05% and $CaCO_3$ 0.3% (pH 7.0)). The flasks were shaken on a rotary shaker (170 r.p.m.) at 30 °C for 4 days. The seed culture (3 ml) was transferred into 500-ml Erlenmeyer flasks each containing 100 ml of A3MP production medium (glucose 0.5%, glycerol 2%, soluble starch 2%, pharmamedia (Archer Daniels Midland Company, Lubbock, IL, USA) 1.5%, yeast extract 0.3%, HP-20 (Mitsubishi Chemical Co., Kanagawa, Japan) 1% and Na_2HPO_4 1%). The pH of the medium was adjusted to 8.0 before sterilization. The flasks were shaken on a rotary shaker (170 r.p.m.) at 30 °C for 6 days.

Extraction and isolation

At the end of the fermentation period, 100 ml of EtOAc was added to each flask, and the mixtures were shaken for 1 h. The mixture was centrifuged at 5000 r.p.m. for 10 min, and the organic layer was separated from the aqueous layer containing the mycelium. Evaporation of the solvent gave 3.9 g of extract from 12 L of culture. The crude extract (3.9 g) was partitioned between 10%

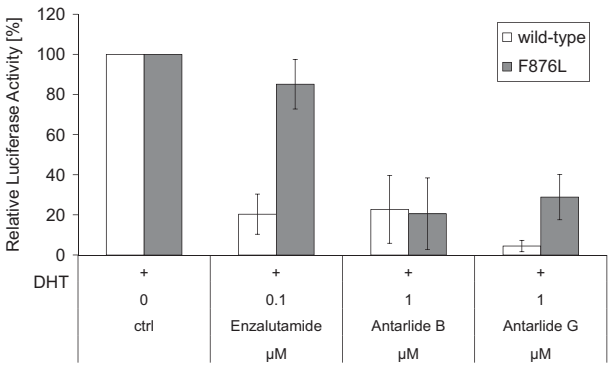

Figure 4 Effect of antarlides B and G on transcriptional activity of wild-type or mutant (F876L) AR.

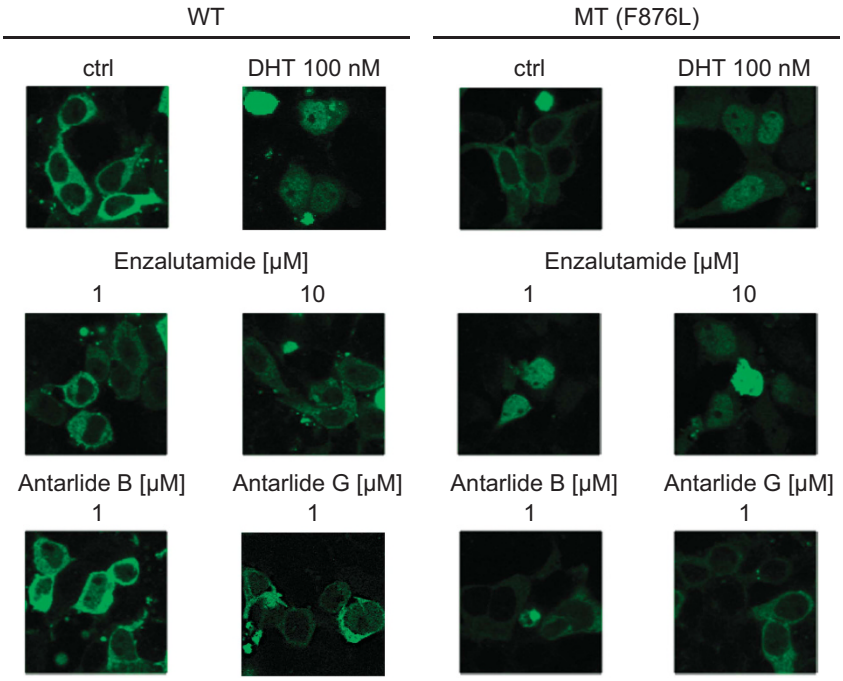

Figure 5 Effect of antarlides B and G on nuclear translocation of wild-type or mutant (F876L) AR.

aqueous MeOH (1.5 L) and *n*-hexane (1.5 L × 3), the former of which was further separated between EtOAc (1.5 L) and H_2O (pH 10) (1.5 L × 3). The EtOAc-soluble fraction (1.6 g) was fractionated by centrifugal liquid–liquid partition chromatography (CPC; Senshu Scientific Co. Ltd., Tokyo, Japan; CPC240 apparatus) with $CHCl_3$-MeOH-H_2O (pH 9) (5:6:4, lower phase stationary). The active stationary phase (737 mg) was repeatedly purified by reverse-phase C30 column (Develosil C30-UG-5; Nomura Chemical, Aichi, Japan) chromatography with MeCN/H_2O (11:9). The fraction containing antarlides F–H was evaporated, and the remaining aqueous solution was extracted with EtOAc. The organic layer was then concentrated. Final purification was achieved by preparative C30 column chromatography with MeOH/H_2O (3:1). The fraction containing antarlides F–H was evaporated, and the remaining aqueous solution was extracted with EtOAc. The organic layer was then concentrated to give a antarlide F (2.2 mg), antarlide G (1.6 mg) and antarlide H (1.0 mg). Note that all isolation steps were carried out in the dark, because antarlides F–H are unstable under room light.

Antarlide F

Pale yellow powder; $[\alpha]^{22}_D$ +125 (*c* 0.1, MeOH); UV (MeOH) λ_{max}(log) 237 (4.56), 332 (4.28) nm; IR (cm^{-1}) 3393, 1685; ^1H and ^{13}C NMR data, see Table 1; HR-ESITOF MS $[M-H]^-$ 535.3062 (calcd for $C_{33}H_{43}O_6$, 535.3060).

Antarlide G

Pale yellow powder; $[\alpha]^{22}_D$ +209 (*c* 0.1, MeOH); UV (MeOH) λ_{max}(log) 235 (4.48), 335 (4.14) nm; IR (cm^{-1}) 3363, 1684; ^1H and ^{13}C NMR data, see Table 1; HR-ESITOF MS $[M-H]^-$ 535.3061 (calcd for $C_{33}H_{43}O_6$, 535.3060).

Antarlide H

Pale yellow powder; $[\alpha]^{22}_D$ +51 (*c* 0.1, MeOH); UV (MeOH) λ_{max}(log) 237 (4.76), 335 (4.35) nm; IR (cm^{-1}) 3370, 1685; ^1H and ^{13}C NMR data, see Table 1; HR-ESITOF MS $[M-H]^-$ 535.3061 (calcd for $C_{33}H_{43}O_6$, 535.3060).

Photoisomerization of antarlides A–H

A solution of antarlides A–H (0.5 mg ml^{-1}) in MeOH was exposed to room light in a capped clear microfuge tube. After irradiation, each solution was analyzed by an LC-photodiode array-MS system (Waters) with a photodiode array detector (2996) and mass analyzer (Micromass ZQ; Waters).

[^{3}H]DHT-AR *in vitro* binding assay

This assay was performed according to the method described previously. In brief, the gene sequence corresponding to the ligand-binding domain (LBD, amino acids 609–919) of the C terminus of AR was expressed in *Escherichia coli* strain DH5α as a maltose-binding protein-fused protein (MBP-LBD), followed by purification using amylose resin (Bio-Rad Laboratories, Hercules, CA, USA). The resulting purified recombinant MBP-LBD (50 μg ml^{-1}), [^{3}H] DHT (2 nM) and test samples were incubated at 4 °C for 3 h. [^{3}H] DHT-bound MBP-LBD then was precipitated with hydroxyapatite, and radioactivity was measured using a liquid scintillation counter.

[^{3}H] Estradiol-ER *in vitro* binding assay

The gene sequence corresponding to the LBD (amino acids 301–551) of the C terminus of ER was expressed in *Escherichia coli* strain DH5α as an MBP-LBD, followed by purification using amylose resin (Bio-Rad Laboratories). The resulting purified recombinant MBP-LBD (50 μg ml^{-1}), [^{3}H] estradiol (1 nM) and test samples were incubated at 4 °C for 15 min. [^{3}H] Estradiol-bound MBP-LBD then was precipitated with hydroxyapatite, and radioactivity was measured using a liquid scintillation counter.

Luciferase reporter assay

Human embryonic kidney 293T cells were plated at 3.5×10^5 cells per well in 6-well plates and incubated in RPMI medium supplemented with 10% fetal bovine serum for 24 h. The cells were transfected with 0.1 μg of pTri-AR expression construct, 1 μg of PSA enhancer/promoter-Luc and 10 ng of control plasmid pCAGGS-lacZ for normalization of transfection efficiency using Lipofectamine (Invitrogen, Carlsbad, CA, USA). Transfection medium was removed 24 h later and replaced with RPMI-1640 medium containing 2% charcoal-stripped serum. The cells were then treated with DHT (100 nM) and test samples. After 24 h, cells were harvested and assayed for luciferase activity and β-galactosidase activity with the *lacZ* reporter gene assay system (Roche, Mannheim, Germany).

Nuclear translocation of AR

Human embryonic kidney 293T cells were plated at 1.00×10^6 cells per dish in 10-cm dishes and incubated in RPMI medium supplemented with 10% fetal bovine serum for 24 h. The cells were transfected with 7.5 μg of EGFP-AR

expression construct using Lipofectamine (Invitrogen). Transfection medium was removed 24 h later and the cells were reseeded at 1.0×10^5 cells per well in 12-well plates and incubated in RPMI medium supplemented with 10% fetal bovine serum for 24 h. The cells were treated with DHT (100 nM) or test samples. After 1 h, cells were fixed with 3% paraformaldehyde in phosphate-buffered saline at room (ambient) temperature and observed under a confocal laser scanning microscope system FV1000 (Olympus Corp., Tokyo, Japan).

CONFLICT OF INTEREST

The authors declare no conflict of interest.

ACKNOWLEDGEMENTS

This work was partly supported by MEXT KAKENHI Grant Number JP23102006 (to MI) and JSPS KAKENHI Grant Number JP 15H03116 (to MI). We thank Prof. Kiyotake Suenaga (Keio University) for providing information on the NMR spectroscopic analysis.

1 Jemal, A. *et al.* Cancer statistics, 2008. *Cancer J. Clin.* **58**, 71–96 (2008).
2 Heinlein, C. A. & Chang, C. Androgen receptor in prostate cancer. *Endocr. Rev.* **25**, 276–308 (2004).
3 Chen, C. D. *et al.* Molecular determinants of resistance to antiandrogen therapy. *Nat. Med.* **10**, 33–39 (2004).
4 Azad, A. A. *et al.* Androgen receptor gene aberrations in circulating cell-free DNA: biomarkers of therapeutic resistance in castration-resistant prostate cancer. *Clin. Cancer Res.* **21**, 2315–2324 (2015).
5 Tran, C. *et al.* Development of a second-generation antiandrogen for treatment of advanced prostate cancer. *Science* **324**, 787–790 (2009).
6 Korpal, M. *et al.* An F876L mutation in androgen receptor confers genetic and phenotypic resistance to MDV3100 (enzalutamide). *Cancer Discov.* **3**, 1030–1043 (2013).
7 Saito, S., Fujimaki, T., Panbangred, P., Igarashi, Y. & Imoto, M. Antarlides: a new type of androgen receptor (AR) antagonist that overcomes resistance to AR-targeted therapy. *Angew. Chem. Int. Ed.* **55**, 2728–2732 (2016).
8 Bax, Ad., Farley, K. A. & Walker, G. S. Increased HMBC sensitivity for correlating poorly resolved proton multiplets to carbon-13 using selective or semi-selective pulses. *J. Magn. Reson.* **119**, 134–138 (1996).
9 Yu, L. *et al.* Jomthonic acids B and C, two new modified amino acids from *Streptomyces* sp. *J. Antibiot.* **67**, 345–347 (2014).

Supplementary Information accompanies the paper on The Journal of Antibiotics website (http://www.nature.com/ja)